Simulation of Tack Welding Procedures in Butt Joint Welding of Plates

Tack welding procedure influences variation in root opening during automatic welding

BY M. JONSSON, L. KARLSSON AND L-E. LINDGREN

ABSTRACT. In butt joint welding of plates, the change in root opening in front of the welding arc is of great importance. In order to automate the welding process, one must know how the change in root opening is affected by welding variables and plate configuration. The most important welding variables are the welding speed and the arc energy per unit length of the weld. The configuration is dependent on the material of the plates, their size, their restraints and the tack welding procedure. In this paper, the influence of the tack welding procedure on the change in root opening was investigated. This change during the first part of welding depends on the order in which the tack welds are made. It is also affected by the starting position of the welding arc. These effects were studied in seven theoretical analyses—three cases where the tack welding procedures differed and four cases where the temperature fields at the beginning of the butt joint welding differed. In two of the cases, theoretical results were compared with experiments. In the theoretical analyses, the finite element method was used. It was found that the change in root opening during the first part of welding is strongly dependent on the tack welding procedure.

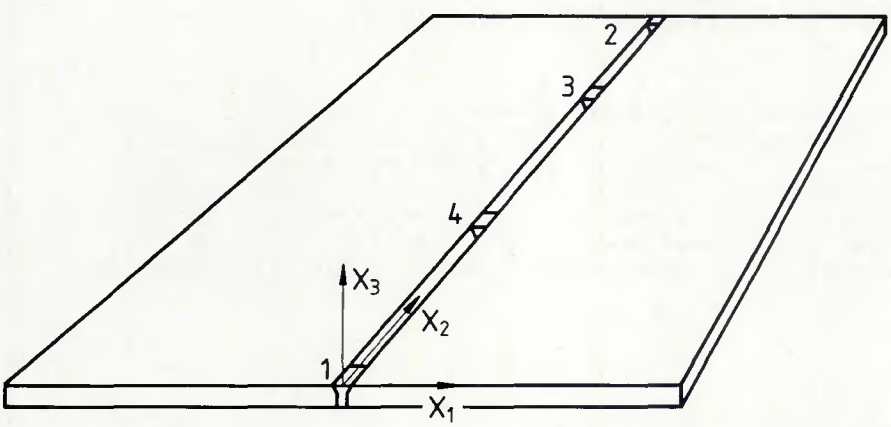

Fig. 1—Butt joint welded plate to be analyzed. Heat source starts at $x_2 = 0$ and moves along x_2 axis with constant velocity

Introduction and Background

In automatic butt joint welding, it is important to know the deflections of the plates during the welding process. In particular, the change in root opening (Δg) in front of the moving arc between the tack welded plates is of interest. If the root opening closes, complete penetration may not be achieved. If the joint clearance opens, the root face may melt away, letting weld metal drop through. The change in root opening depends on the welding variables, the tack welding, the restraints of the plates and the size of the plates. The most important welding variables are the arc energy per unit length of the weld and the welding speed.

In Ref. 1, simulation of automatic one pass welding was presented. The simulation included the tack welding, the butt joint welding and the cooling of the plates to ambient temperature. The transient temperature fields and the associated strain and stress fields were calculated. Also, the change in root opening in front of the moving arc during welding was calculated. The finite element (FE-) method was used in calculations. The main object in Ref. 1 was to verify the mathematical model simulating the welding process.

M. JONSSON, L. KARLSSON and L-E. LINDGREN are with the Department of Mechanical Engineering, Lulea University of Technology, Lulea, Sweden.

Two different experiments were performed in Ref. 1. In one of these two experiments, two tack welded plates of the size 0.5 × 1.0 × 0.01 m (1.6 × 3.3 × 0.03 ft) were welded in an automatic gas metal arc welding process with the gross heat input at 1.6 MJ/m (40,640 J/in.)—Fig. 1. The arc efficiency was estimated to be 0.72. The welding started at $x_2 = 0$ and time $t = 0$. The welding arc moved along the x_2 axis with a constant velocity $v = 0.005$ m/s (0.20 in./s). The tack welds are denoted 1, 2, 3 and 4. These numbers also give the order in which the tack welds were made. The length of each tack weld was 30 mm (1.2 in.). The change in root opening was measured with a video camera which was attached to the welding device. The video camera recorded the gap 0.12 m (4.7 in.) in front of the moving arc. The change in root opening was determined by taking the difference between the opening during and before butt joint welding (but after the tack welding). The method for recording the root opening is shown in Fig. 2. The camera and the mirror move with the welding torch.

A detailed account of deformations and stresses in welding is given in the state-of-the-art article noted in Ref. 2. In Ref. 3, the change in root opening was studied for different sizes of plates.

In this paper, the change in root opening is studied for three different tack welding procedures, case 1 to case 3. In four other cases, case 4 to case 7, the influence of different temperature fields at the beginning of the welding is studied. These four simulations were performed in order to investigate how the change in root opening during the first part of the butt joint welding is influenced by the heating of tack weld 1—Fig. 1. Tack weld 1 was melted completely in case 4. In cases 5 to 7 the temperature in tack weld 1 was reduced during the first 20 s of welding. This may describe what happens in a real welding situation where the arc starts at some distance from the edge rather than at the edge $x_2 = 0$.

In each of the first three cases, tack welding and subsequent butt joint welding of two plates of the same size were simulated. Plate size after welding in these cases was 1.0 × 1.0 × 0.01 m (3.3 × 3.3 × 0.03 ft). In case 1 and case 2, the tack welds were made in the order 1, 2, 3 and 4. In case 1, the welding of the tack welds 3 and 4 started when the temperatures in the tack welds 1 and 2 were about 250°C (482°F). In case 2, the temperatures were about 20°C (68°F) in tack welds 1 and 2, when the welding of tack weld 3 started. In case 3, the tack welds were made in the order 4, 3, 2 and 1. The temperatures in the tack welds 4 and 3 were about 250°C (482°F) when the welding of tack weld 2 started. Case 1 is taken from Ref. 1 where the change in root opening was studied both experi-

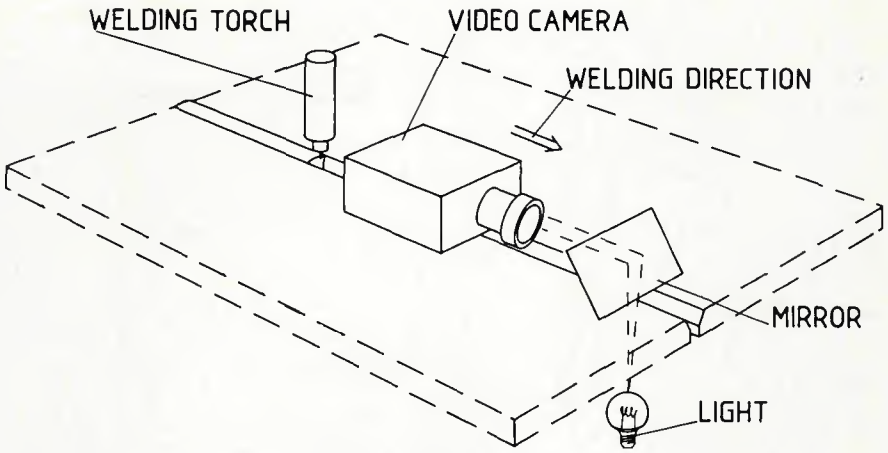

Fig. 2—Camera set-up for measuring root opening (figure courtesy of John Wiley & Sons, Ltd., reprinted from Numerical Methods in Heat Transfer-*Vol. 3)*

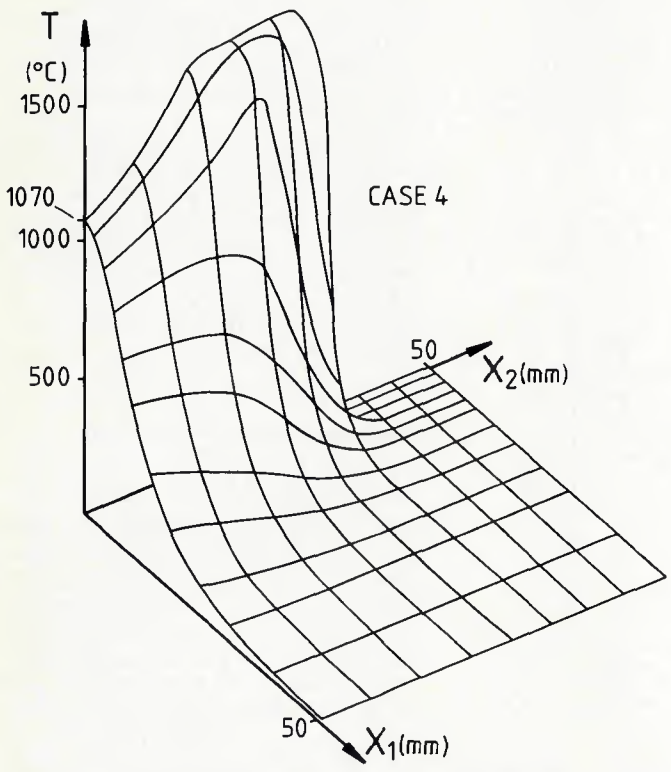

Fig. 3—Temperature field at beginning of welding for case 4

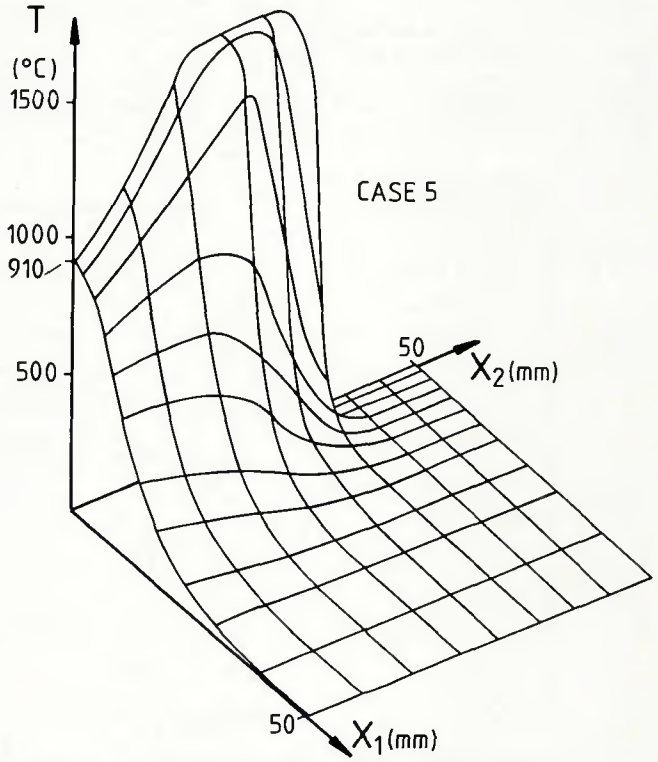

Fig. 4—Temperature field at beginning of welding for case 5

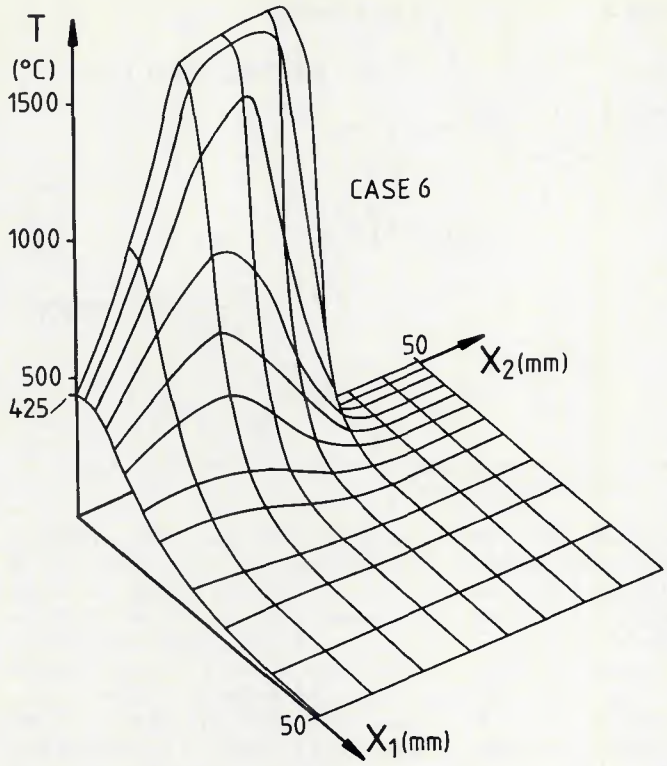

Fig. 5 – Temperature field at beginning of welding for case 6

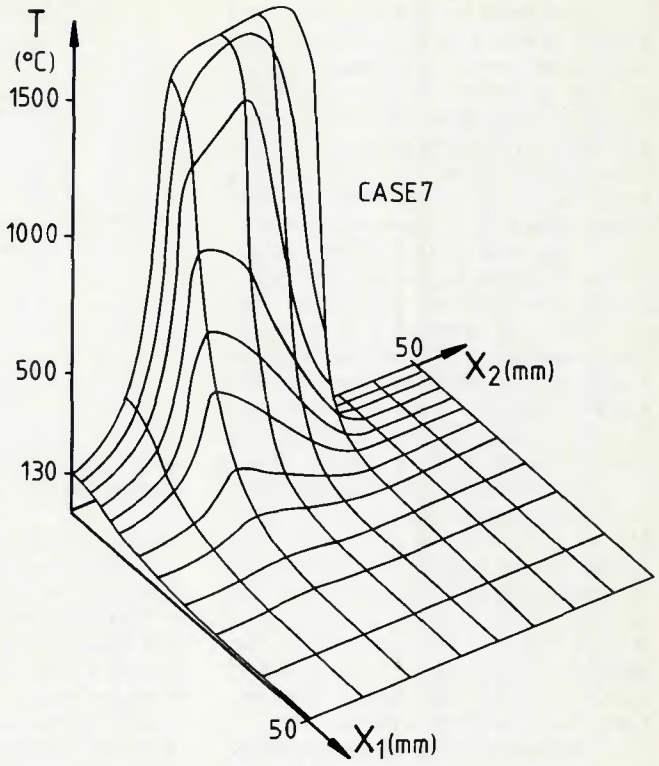

Fig. 6 – Temperature field at beginning of welding for case 7

mentally (as described above) and theoretically. In cases 2 and 3, only theoretical studies were performed. The welding variables given above for the experiment in Ref. 1 were used in the theoretical analyses in case 1 to case 3.

In each of case 4 to case 7, two plates of size 0.2 × 1.0 × 0.01 m (0.7 ×3.3 × 0.03 ft) were first tack welded and then finally butt joint welded along the x_2 axis. The tack welds were made in the order 1, 2, 3 and 4 in these four cases. Case 4 is taken from Ref. 2 where the change in root opening was studied both experimentally and theoretically. The same welding procedure and welding variables as were used in case 1 were used in case 4. In cases 5 to 7, the temperatures in tack weld 1 and its vicinity were reduced during the first 20 s of welding. The change in root opening in these cases was studied theoretically only during the first 60 s of welding. The four different temperature fields used in cases 4 to 7 are shown in Figs. 3, 4, 5 and 6, respectively, at 7.5 s after the start of welding.

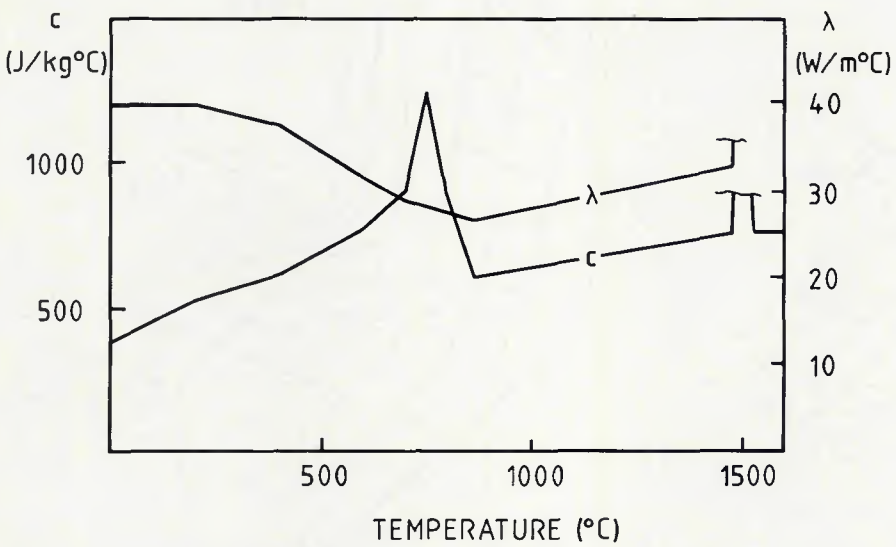

Fig. 7 – Thermal conductivity λ and heat capacity c for the fine grain steel used as a function of temperature noted in Ref. 4

Thermal Analysis

The material investigated is a fine-grain steel with a yield stress of 360 MPa (52,200 psi) at room temperature. The filler material used was ESAB 1.2/12.51 (AWS ER70S-6). The temperature-dependent thermal properties used in Ref. 1 and in this paper were taken from Ref. 4. They are shown in Fig. 7. Uniform properties were assumed through the plate thickness.

The temperature fields and the mechanical fields were assumed to be thermodynamically uncoupled (Ref. 1). The heat content (enthalpy) was used as a dependent variable in the heat conduction equation. The finite element method (FEM) was used in the analysis. Owing to symmetry, only one half of the plate need be analyzed.

Temperature Calculations in Tack Welding

Temperature fields due to tack welding were calculated in the cases 1 to 4. For the cases 5 to 7, the temperature field due to tack welding was the same as for case 4. The x_1x_2 plane was divided into 5600 lowest-order triangular elements. Convective surface heat transfer was simulated by heat sinks according to Ref. 1. The calculation for case 1 started with the heat input simulating tack welds 1 and 2. The heat input was applied during a few seconds. After 60 s, the heat input simulating tack weld 3 was applied and

the heat input for tack weld 4 was applied after another 60 s. The temperatures in tack welds 1 and 2 were about 250°C (482°F) when tack weld 3 was made. In case 2, tack welds 1 and 2 had cooled to room temperature of 20°C (68°F), when the welding of tack weld 3 started. In case 3, the calculation started with the heat input simulating the tack welds 4 and 3. The heat input was applied during a few seconds. After 60 s, the heat input simulating tack weld 2 was applied and the heat input for tack weld 1 was applied after another 60 s. The temperatures in tack welds 3 and 4 were about 250°C (482°F) when tack weld 2 was made. The tack welding procedure in cases 4 to 7 was the same as in case 1 described above.

Temperature Calculations in Butt Joint Welding

The welding speed v used was high enough to allow the heat flow along the weld to be neglected as compared to the heat flow transverse to the weld. This approximation was shown in Ref. 1 to be very accurate. In Ref. 1, the two-dimensional temperature fields for the x_1x_2 plane were calculated from one-dimensional temperature fields from the x_1x_3 plane, as noted in Ref. 5.

$$T(x_1,x_2,t) = T_1(x_1, t-(x_2/v)) \quad \text{for } x_2 - vt \le 0$$
$$= 20°C \quad \text{for } x_2 - vt > 0$$

In the calculation of $T_1(x_1,t')$ ($t' = t - (x_2/v)$), the x_1x_3 plane was divided into 150 lowest-order triangular elements. The finite element mesh can be seen in Fig. 8. It should be noted that each triangle in Fig. 8 represents four triangular finite elements. The heat input was simulated by a line heat source along the x_3 axis. The strength of the heat source was constant across the plate thickness and the heat source was turned on for three seconds. Convective surface heat transfer for the upper and lower surfaces and the edge $x_1 = 0.500$ m (1.6 ft) was included. Due to symmetry, the edge $x_1 = 0$ was adiabatic when the heat input was terminated. The temperature fields $T_1(x_1,t')$ were computed as the average temperature for a given x_1 coordinate. The calculated and measured temperatures at $(x_1,x_2) = (10,510)$ mm and $(x_1, x_2) = (30,585)$ mm are shown in Fig. 9. As can be noted in Fig. 9, the measured temperature is constant at room temperature until the arc passes the measuring point and then rises very quickly. This shows that it is appropriate to neglect the heat conduction along the weld.

The temperature calculations in this paper were performed as described above in all seven cases except in cases 5 to 7 where the temperatures in tack weld 1 and its vicinity were reduced during the first 20 s of welding. This reduction was changed linearly so that the temperatures in cases 5 to 7 reached the temperatures of case 4 after 20 s. This reduction was made in order to study situations where tack weld 1 was not fully melted.

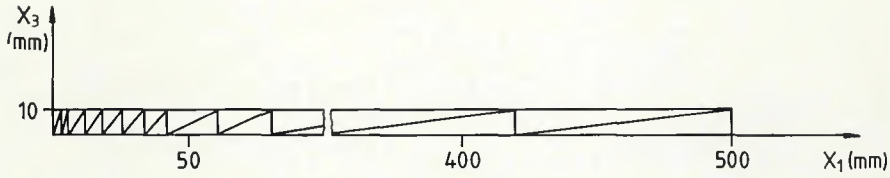

Fig. 8 — Finite element mesh for computing $T_1(x_1,t')$. Note that each triangle was divided into the four lowest order triangular elements in the analysis (figure courtesy of John Wiley & Sons, Ltd., reprinted from Numerical Methods in Heat Transfer — *Vol. 3)*

Mechanical Analysis

Plane stress conditions were assumed and a thermo-elastoplastic material model was used (Ref. 1).

Volume changes due to phase transformations were accounted for by the thermal dilatation diagram in Fig. 10. The curves in Fig. 10 were based on $\Delta t_{8/5}$, which is the time for cooling from 800°C to 500°C (1472–932°F). In this study, $\Delta t_{8/5}$ was calculated to be 22 s. This cooling time was about the same for the entire heat affected zone where the phase transformations occur. During heating, the top curve in the dilatation diagram was followed. Depending on the maximum temperatures reached, different curves were followed during cooling.

Beside ϵ^T, the following material parameters are needed for the mechanical analysis, elastic modulus E, Poisson's ratio ν, yield stress for the base material σ_{yb} and for the filler material σ_{yf}. The hardening moduli were set to zero. However, in order to account for some hardening, σ_{yf} was chosen to be 450 MPa (65,250 psi) at room temperature in the analysis. The temperature dependence of E, σ_{yb}, and ν was taken from Ref. 4. E, σ_{yb}, σ_{yf} and ν are shown as functions of temperature in Fig. 11.

In the mechanical analyses, the x_1x_2 plane was divided into 700 triangular finite elements with cubic base functions — Fig. 12. The system had about 4200 degrees of freedom. One line of elements along the x_2 axis was used for simulation of the free edge of the weld. The elements in this line had a width of 2 mm (0.08 in.) in the x_1 direction. The nodal points along the x_2 axis (at $x_1 = 0$) were locked in the x_1 direction. In order to simulate the free edge, these elements were given a very low value of the elastic modulus in front of the moving arc. At the location of the tack welds in front of the moving arc and behind the moving arc, the elements were given values of the temperature-dependent elastic modulus according to Fig. 11.

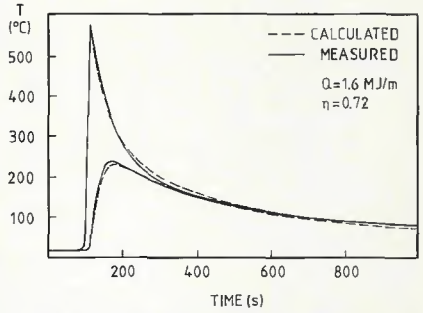

Fig. 9 — Calculated and measured temperatures at $x_1 = 10$ mm, $x_2 = 510$ mm and $x_1 = 30$ mm, $x_2 = 585$ mm as a function of time (figure courtesy of John Wiley & Son, Ltd., reprinted from Numerical Methods in Heat Transfer — *Vol. 3)*

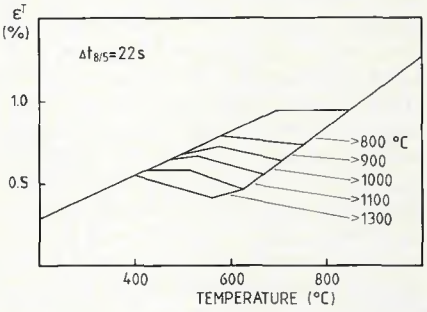

Fig. 10 — Thermal dilatation ϵ^T for the fine grain steel used as noted in Ref. 1 (figure courtesy of John Wiley & Son, Ltd., reprinted from Numerical Methods in Heat Transfer — *Vol. 3)*

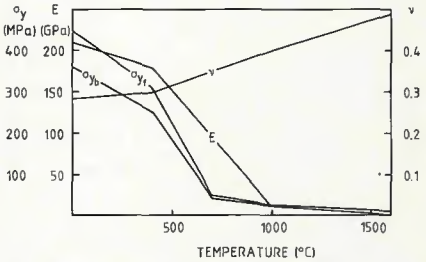

Fig. 11 — Assumed mechanical properties for the fine grain steel used as a function of temperature (figure courtesy of John Wiley & Son, Ltd., reprinted from Numerical Methods in Heat Transfer — *Vol. 3)*

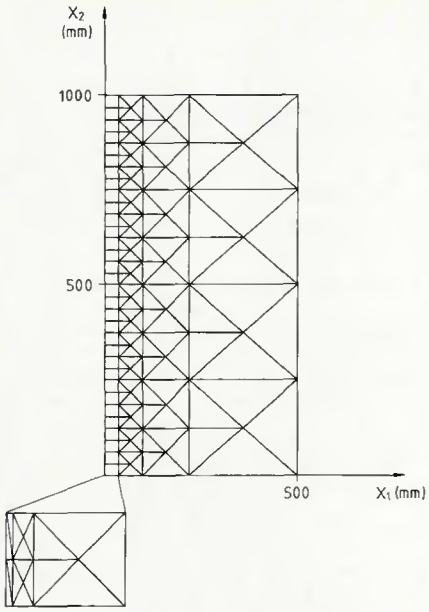

Fig. 12—Finite element mesh used in the analysis. The mesh has 700 triangular elements with cubic base functions

Mechanical Analysis of Tack Welding

Residual stresses after tack welding were calculated for the cases 1 to 4. It was found that the influence from the tack welding on the residual stresses after butt joint welding is negligible. The residual stresses after tack welding in cases 5 to 7 were the same as in case 4. The mechanical analyses of the tack welding started at the time when the third tack weld was made. Thus, two tack welds were present when these analyses started. The reason for this was to avoid ill-conditioned systems of equations. This simplification did not affect the simulations since the stresses obtained after the two first tack welds were made were negligible as compared to those stresses that occurred after the two final tack welds were made. The mechanical analysis of case 1 started with the simulation of the welding of tack weld 3 when the temperatures in tack welds 1 and 2 were about 250°C (482°F). The analysis continued with simulation of tack weld 4. In case 2, the mechanical analysis started with the simulation of tack weld 3 when tack welds 1 and 2 had cooled to room temperature. The mechanical analysis of case 3 started with the simulation of tack weld 2 when the temperatures in tack welds 3 and 4 were about 250°C (482°F). The analysis continued with the simulation of tack weld 1. The order 1, 2, 3 and 4 of the tack welds (in cases 1, 2, 4, 5, 6 and 7) gives compressive residual stresses transverse to the weld in tack welds 1 and 2 and tensile stresses transverse to the weld in tack welds 3 and 4. The magnitudes of the compressive stresses in tack welds 1 and 2 and the tensile stresses in tack welds 3 and 4 are larger in case 2 than in case 1. This is due to the lower temperatures in the tack welds 1 and 2 for case 2 as compared to case 1 when the welding of tack weld 3 started. The order 4, 3, 2 and 1 of the tack welds gives tensile residual stresses transverse to the weld in case 3 in tack welds 1 and 2 and compressive residual stresses transverse to the weld in tack welds 3 and 4. The magnitude of the largest average residual stress after tack welding was in case 1 about 200 MPa (29,000 psi), in case 2 about 250 MPa (36,250 psi) and in case 3 about 100 MPa (14,500 psi).

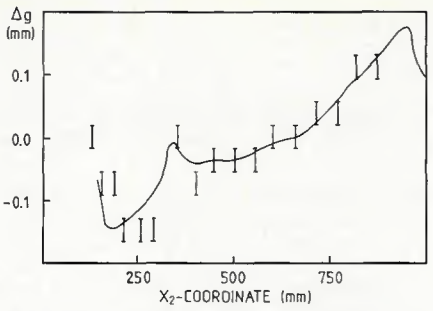

Fig. 13—Case 1. Calculated and measured change in root opening for tack welded plate of size 1.0 X 1.0 X 0.01 m. Measured values fall within length of vertical lines

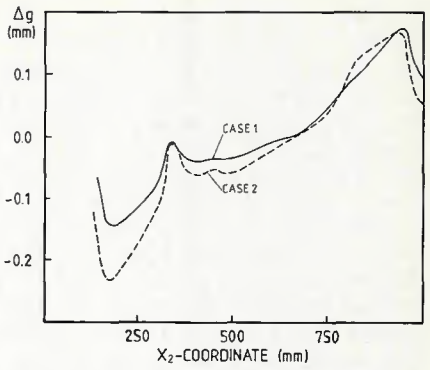

Fig. 14—Cases 1 and 2. Calculated change in root opening for tack welded plates of size 1.0 X 1.0 X 0.01 m. Solid line shows Δg for case 1 and dashed line shows Δg for case 2

Mechanical Analysis of Butt Joint Welding

In the simulations of welding the joint, the residual stress fields after tack welding were used as initial stress fields in all seven cases.

In the cases 1 to 4, the mechanical analyses of the welding were performed for times t = 0 to t = 40,000 s using about 100 time (load) increments for simulation of the welding process and about 20 time (load) increments for simulation of the cooling process.

The mechanical analyses of the welding for the cases 5 to 7 were performed for times t = 0 to t = 60 s.

The change in root opening was calculated 0.12 m (4.7 in.) in front of the moving heat source in all seven cases. It

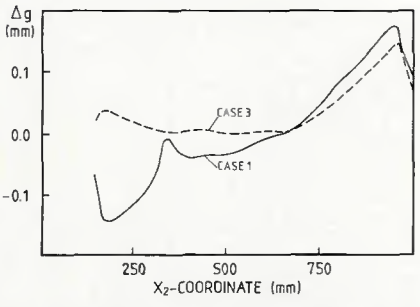

Fig. 15—Cases 1 and 3. Calculated change in root opening for tack welded plates of size 1.0 X 1.0 X 0.01 m. Solid line shows Δg for case 1 and dashed line shows Δg for case 3

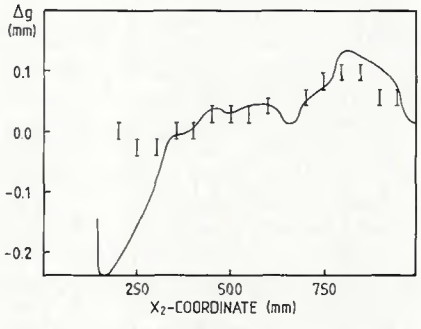

Fig. 16—Case 4. Calculated and measured change in root opening for tack welded plate of size 0.4 X 1.0 X 0.01 m. Measured values fall within length of vertical lines

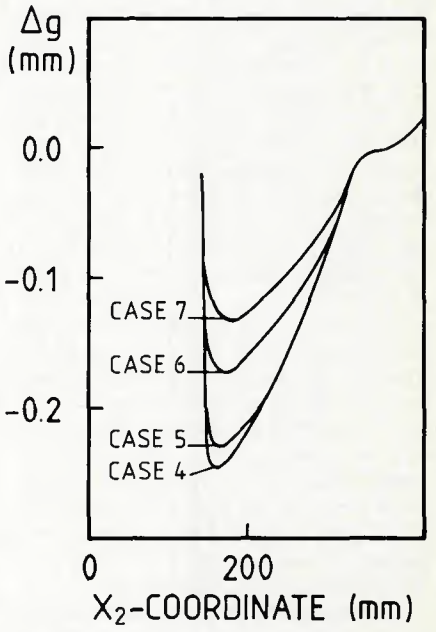

Fig. 17—Cases 4 to 7. Calculated change in root opening 0.12 m in front of the moving arc for four different temperature fields at beginning of butt joint welding of tack welded plate of size 0.4 X 1.0 X 0.01 m

was taken as twice the difference between calculated transverse displacements 2 mm (0.08 in.) from the line of symmetry during the welding and the corresponding displacement at the start of the welding.

Change in Root Opening for Three Different Tack Welding Procedures—Cases 1 to 3

The calculated and measured change in root opening for case 1 is shown in Fig. 13. The results in Fig. 13 are taken from Ref. 1. Calculated changes in root opening for cases 1 and 2 are shown in Fig. 14. In Fig. 15, calculated change in root opening is shown for cases 1 and 3.

Change in Root Opening for Four Different Temperature Fields at the Beginning of Butt Joint Welding—Cases 4 to 7

The calculated and measured change in root opening for case 4 is shown in Fig. 16. The results in Fig. 16 are taken from Ref. 3. The results of case 4 are in Fig. 17 compared to the cases 5 to 7 where the temperature fields at the beginning of the butt joint welding were reduced.

Conclusion

It is seen in Fig. 15 that the change in root opening during the first part of the welding depends strongly on the order in which the tack welds are made. One can therefore conclude that it is possible to estimate the change in root opening during the first part of the butt joint welding with knowledge of the tack welding procedure. In Fig. 14, it is seen that the decrease in root opening is larger in case 2 than in case 1. This is due to the larger tensile forces in tack welds 3 and 4 and the larger compressive force in tack weld 1 in case 2. In order to reduce the magnitude of these forces, the tack welding procedure should be performed as fast as possible.

In Fig. 17, it is noted that the decrease in root opening for cases 5, 6 and 7 is still significant, as compared to case 4, although tack weld 1 was not fully melted in these cases. This may be explained by the large compressive forces in tack weld 1 at the start of the welding. It can be concluded that the difference between calculated and measured values in Fig. 16 cannot be fully explained by a low temperature in tack weld 1 at the beginning of welding.

Acknowledgments

Dr. B.A.B. Andersson, The Aeronautical Institute of Sweden, and ASEA AB are thanked for putting the computer program for thermal and elastoplastic analysis at our disposal. The project was financially supported by the Swedish Board for Technical Development (STU).

References

1. Jonsson, M., Karlsson, L. and Lindgren, L-E. 1985 (April). Deformations and stresses in butt-welding of large plates. In R.W. Lewis and K. Morgan (eds.), *Numerical Methods in Heat Transfer – Volume III,* Wiley.

2. Karlsson, L. 1985 (August/September). Thermal stresses in welding. In R. Hetnarski (ed.), *Thermal Stresses, Volume 1,* North-Holland.

3. Lindgren, L-E., Jonsson, M. and Karlsson, L. 1984. Plate motion in butt-welding of tack-welded plates. *International Conference on Numerical Methods for Transient and Coupled Problems,* July 9–13, Venice, Italy.

4. Andersson, B.A.B. 1978. Thermal stresses in a submerged-arc-welded joint considering phase transformations. *J. Eng. Mat. Tech. (ASME),* 100: 356–362.

5. Andersson, B. and Karlsson, L. 1981. Thermal stresses in large butt-welded plates. *J. Thermal Stresses,* 4 (3–4):491–500.

WRC Bulletin 301
January 1985

A Parametric Three-Dimensional Finite Element Study of 45 Degree Lateral Connections
By P. P. Raju

This bulletin contains a summary of three-dimensional finite element studies carried out on four lateral configurations subjected independently to internal pressure, external in-plane moment on the nozzle, and external in-plane moment on the run pipe. Stress indices for various critical regions are summarized.

Publication of this report was sponsored by the Task Group on Laterals that reported to the Subcommittee on Reinforced Openings and External Loadings and the Subcommittee on Piping Pumps and Valves of the Pressure Vessel Research Committee of the Welding Research Council.

The price of WRC Bulletin 301 is $14.00 per copy, plus $5.00 for postage and handling. Orders should be sent with payment to the Welding Research Council, Room 1301, 345 E. 47 St., New York, NY 10017.

WRC Bulletin 300
December 1984

Under the direction of the Steering Committee on Piping Systems of the Pressure Vessel Research Committee of the Welding Research Council, the Technical Committee on Piping Systems developed a document on criteria establishment describing their objectives and accomplishments, and three technical position documents that have an effect on the design of piping systems, entitled: 1) Technical Position on Criteria Establishment; 2) Technical Position on Damping Values for Piping Interim Summary; 3) Technical Position on Response Spectra Broadening; and 4) Technical Position on Industry Practice.

The Technical Position Documents have been submitted to the ASME Boiler and Pressure Vessel Code Committee and the U. S. Nuclear Regulatory Commission for their use.

The price of WRC Bulletin 300 is $14.00 per copy, plus $5.00 for postage and handling. Orders should be sent with payment to the Welding Research Council, Rm. 1301, 345 E. 47 St., New York, NY 10017.

WRC Bulletin 298
September 1984

Long-Range Plan for Pressure-Vessel Research—Seventh Edition
By the Pressure Vessel Research Committee

Every three years, the PVRC Long-Range Plan is updated. The Sixth Edition was widely distributed for review and comment. Updated problem areas have been suggested by ASME, API, EPRI and other organizations. Most of the problems in the Sixth Edition have been modified to meet current needs, and a number of new problems have been added to this Seventh Edition.

The list of "PVRC Research Problems" is composed of 58 research topics, divided into three groups relating to the three divisions of PVRC; i.e., materials, design and fabrication. Each project is outlined briefly in a project description, giving the title, statement of problem and objectives, current status and action proposed.

Because of budget limitations, PVRC will not be able to investigate all of these problems in the foreseeable future. Therefore, the cooperation and efforts of other groups in studying these areas is invited. If work is planned on one of the problems, PVRC should be informed in order to avoid duplication.

Publication of this bulletin was sponsored by the Pressure Vessel Research Committee of the Welding Research Council. The price of WRC Bulletin 298 is $14.00 per copy, plus $5.00 for postage and handling. Orders should be sent with payment to the Welding Research Council, Room 1301, 345 E. 47th St., New York, NY 10017.

WRC Bulletin 296
July 1984

Fitness-for-Service Criteria for Pipeline Girth-Weld Quality
By R. P. Reed, M. B. Kasen, H. I. McHenry, C. M. Fortunko and D. T. Read

In this report, criteria have been developed for applying fitness-for-service analyses to flaws in the girth welds of the Alaska Natural Gas Transmission System pipeline. A critical crack-opening-displacement elastic-plastic fracture mechanics model was developed and experimentally modified. Procedures for constructing curves based on this model are provided. A significantly improved ultrasonic method for detecting and dimensioning significant weld flaws was also developed.

Publication of this report was co-sponsored by the National Bureau of Standards and the Weldability Committee of the Welding Research Council. The price of WRC Bulletin 296 is $16.50 per copy, plus $5.00 for postage and handling. Orders should be sent with payment to the Welding Research Council, Room 1301, 345 E. 47 St., New York, NY 10017.